NUCLEAR SCIENCE AND TECHNIQUES **25**, 030502 (2014)

Using Xe as a heavy atom for phase determination of protein trichosanthin structure*

CHEN Ya-Xing (陈亚星),[1] LI Min-Jun (李敏军),[1,†] YU Feng (郁峰),[1] LIU Ke (刘科),[1] XU Chun-Yan (徐春艳),[1] SUN Bo (孙波),[1] ZHOU Huan (周欢),[1] XU Qin (徐琴),[1] and HE Jian-Hua (何建华)[1,‡]

[1] *Shanghai Institute of Applied Physics, Chinese Academy of Sciences, 239 Zhangheng Road, Shanghai 201204, China*

(Received March 4, 2014; accepted in revised form March 13, 2014; published online June 20, 2014)

Under gas pressures of 1–3 MPa, xenon can be bound to discrete sites in hydrophobic cavities of protein, so as to use Xe as a heavy atom for determining phases in protein crystallography. Using single anomalous scattering diffraction method, we demonstrate that an interpretable electron density map can be obtained for protein trichosanthin from a single xenon derivative. We found, for the first time, a pre-existing hydrophobic cavity just under the protein surface of trichosanthin.

Keywords: Xenon, Phasing, SAD, Hydrophobic cavity, Trichosanthin

DOI: 10.13538/j.1001-8042/nst.25.030502

I. INTRODUCTION

Having 54 electrons, a xenon atom belongs to the category of "heavy atoms" in protein crystallography. Although the absorption edges of xenon are located either at short (K edge at 0.358 Å) or long wavelengths (L edges, above 2 Å), the residual anomalous signal at the routinely accessible Cu K_α wavelength (1.54 Å) is sufficiently large to calculate the phase information ($f' = -0.783$, $f'' = 7.348$, http://skuld.bmsc.washington.edu/scatter/data/Xe.html). These suggest that xenon may be useful as a heavy atom for determining phases in protein crystallography.

Xenon has been used in protein crystallography since the 1960s, as a method for obtaining phase information, or an indicator of O_2 binding sites [1]. The pioneering crystallographic studies of Schoenborn and co-workers demonstrated that sperm whale myoglobin [1] and horse haemoglobin [2] crystals can bind xenon under moderate pressure, through weak van der Waals forces. Xenon binds to protein with very little perturbation of the surrounding molecular structure. Therefore, protein-xenon complexes can be used as highly isomorphous heavy-atom derivatives for solving the phase problem in X-ray crystallography [3, 4]. Xenon has now been used successfully as a heavy-atom for the phase determinations of unknown protein structures [5–7]. It is also used as probes to explore the oxygen diffusion channels of different heme proteins [8, 9], hydrophobic cavities [10] and putative ligand migration tunnels inside of various proteins [11, 12].

Trichosanthin (TCS) is a type-I ribosome-inactivating protein that is isolated from the root tuber of the Chinese medicinal herb *Trichosanthes kirilowii* Maxim [13, 14], which exhibits multiple pharmacological properties including abortifacient, antitumor, anti-virus, and especially anti-HIV activities [15, 16]. It was reported that a TCS molecule consists of two $\alpha + \beta$ domains: a large N-terminal domain (residues 1-181) and a small C-terminal domain (residues 182–247) [17, 18]. Recently, we find that TCS crystals grow on a mica surface in an epitaxial growth way induced by lattice of the mica substrate [19]. This indicates that TCS has the potential of acting as a fusion tag to help crystal growth of the chimeric proteins, which cannot succeed in conventional crystallization strategies.

In this report, we successfully added xenon gas into the crystals of recombinant trichosanthin protein under 1–3 MPa. Using the single xenon derivative, the crystal structure of TCS was solved by single-wavelength anomalous diffraction (SAD) method without any known TCS structure information. It demonstrates an interpretable electron density map of xenon atoms inside a hydrophobic cavity of TCS. Compared with the native TCS crystal structure solved in parallel, it is found that the xenon-binding cavity is pre-existing and adjacent to the substrate binding site of this enzyme protein.

II. EXPERIMENTAL SECTION

A. Recombinant protein trichosanthin expression and purification

The cDNA of full-length trichosanthin (TCS) from *T. Kirilowii* was synthesized by GeneWiz Co., Ltd (Suzhou, China). The DNA related to the protein sequence of mature TCS (residues D24-A270) was sub-cloned into the expression vector pET28a to form a fusion protein with His_6 tag and TEV (Tobacco Etch Virus) protease cutting site at its N termini. The constructed plasmid was transformed into expression host strain *E. coli* BL21 (DE3). Cell harboring this expression plasmid was grown in LB broth containing 34 μg/mL kanamycin to mid-log phase at 37 °C. After cooling, the protein was induced by 0.1 mM IPTG at 18 °C for about 18 hours. The cells were harvested and re-suspended in buffer A [100 mM Tris-HCl (pH 7.5, 4 °C), 10% (v/v) glycerol, 100 mM NaCl, 20 mM imidazole] and then were lysed by sonication. The lysate was centrifuged, and the supernatant was loaded on a 10 mL Ni^{2+}-chelating Sepharose column

* Supported by the Major State Basic Research Development Project in China (No. 2011CB911102) and National Natural Science Foundation of China (Nos. 31000389, 31100528 and 31100529)

† liminjun@sinap.ac.cn

‡ hejh@sinap.ac.cn

(GE Healthcare). The column was washed with 200 mL of buffer A and eluted with buffer A with 200 mM imidazole. The eluted fraction was buffer exchanged to remove imidazole with desalting column (GE Healthcare). Self-made recombinant TEV protease was added in the pooled fraction at 20 °C for 12 hours to remove the His_6 tag. The reactant passed through the Ni^{2+}-chelating Sepharose column again to separate the TCS protein from the His6-tagged proteins. The flow-through was applied to a Superdex 75 prep grade gel filtration column (GE Healthcare) to purify the TCS protein to $> 95\%$ pure as judged by SDS/PAGE. The final protein in concentration of $\sim$10 mg/ml was subjected to crystallization.

B. Crystallization and preparation of xenon derivatives

Trichosanthin (TCS) crystallized in reservoir solution with 1.2 M KCl, 100 mM sodium citrate, pH 5.5 at 291 K using hanging-drop vapor-diffusion method. Xenon derivative TCS crystals were prepared at 18 °C by pressurizing TCS crystals using Xenon chamber (Hampton Research). For Xe gas pressurization, a crystal was mounted in a nylon loop from the mother liquor, dipped through cryoprotectant (20% glycerol and 80% reservoir solution), and placed in the pressure chamber. Following incubation (5–10 min), the chamber was depressurized in 10 seconds, and the crystal was flash-frozen in liquid nitrogen in 5 seconds. Pressures tests were conducted at 3, 2, and 1 MPa, in combination with two sets of incubation times (5 and 10 minutes), and 32 crystals were screened for diffraction. Nine complete datasets collected were used for analyses of Xe occupancy, and one was used to solve the phase of TCS by SAD method.

C. Data collection and processing

All diffraction datasets were collected on beamline BL17U1 of Shanghai Synchrotron Radiation Facility (SSRF). The wavelength was 1.54 Å, but one dataset of native TCS was collected at 0.98 Å as control. The datasets were indexed, integrated, and scaled with the HKL2000 package [20]. The data collection statistics for experimental conditions of 3 MPa pressure and 10 min incubation time are given in Table 1.

For SAD phasing solution of the TCS xenon derivative, the anomalous substructure of xenon atom were determined by SHELX C/D [21]. Xe-SAD phasing was calculated by OASIS [22] from the CCP4 suite [23] followed by density improvement in DM [24]. Initial models were built using the build-in Solve/Resolve [25], followed by model extension/rebuilding in ARP/wARP [26]. The model was refined using SAD refinement with optimization of the xenon atom occupancy in REFMAC [27]. For the native TCS dataset, a molecular replacement solution for one TSC molecule in the asymmetric unit was obtained with the reported TCS structure (pdb code: 1TCS [18]) as the search model using Phaser [28]. All final models were produced after several iterative rounds of manual rebuilding in Coot [29] and refinement in Phenix [30].

TABLE 1. Crystal statistics of TCS xenon derivative (TCS/Xe) and native TCS.

Crystal	TCS/Xe	Native TCS
Data Collection		
Wavelength (Å)	1.54	0.98
Temperature (K)	100	100
Resolution ((Å)	1.95	1.01
Measured reflections	31 692	232 654
Unique reflections	17 182	121 102
Redundancy	13.5	13.5
Completeness (%)	99.3	99.7
Mean I/σ	38.6	44.7
Rmerge	0.066	0.067
Space group	$P2_12_12_1$	$P2_12_12_1$
Unit cell parameters		
a (Å)	38.01	37.88
b (Å)	75.38	75.11
c (Å)	78.78	78.42
$\alpha = \beta = \gamma$ (deg)	90.00	90.00
Refinement		
R_{work}	16.6 (15.5)[a]	15.3 (18.3)[a]
R_{free}[b]	20.3 (20.5)[a]	15.8 (19.4)[a]
R.m.s.d from ideality		
Bonds (Å)	0.007	0.008
Angles (deg)	1.020	1.282
Ramachandran plot		
Allowed regions (%)	99.6	99.6

[a] Values in parentheses apply to the highest resolution shell.
[b] R_{free} is the Rfactor based on 5% of the data excluded from refinement.

III. RESULTS AND DISCUSSION

A. The preparation of xenon gas derivatives

Trichosanthin is bio-synthesized as a preproprotein consisting of 289 amino acids [14]. It is further processed to a 247-residue single-chain polypeptide mature form TCS, via removing an N-terminal 23-residue signal peptide and a C-terminal 19-residue propeptide. Not extracted from the plant T. kirilowii, the recombinant TCS protein used in this study was heterogeneously expressed and purified from bacteria *E. Coli* with the same amino acid sequence as the mature TCS. As listed in Table 1, high resolution native crystal diffraction data, $\sim$1.0 Å, were collected from crystals of this batch of protein at SSRF.

High quality TCS crystals were used to prepare Xe derivative crystals using pressurized gas chamber. To avoid the crystals drying out during the gas incubation, a stripe of filter paper soaking with reservoir solution were placed around the chamber wall. The pressurized crystals should be flash-frozen in liquid nitrogen after released from xenon chamber, because the process of xenon binding is completely reversible. Xenon atoms were trapped at the binding sites under cryogenic temperature, so the data were acquired in the same way as with native crystals.

B. Binding site of xenon

A fluorescence excitation scan was performed on-site to verify the presence of xenon anomalous signals in the sample. Because the residual anomalous signal Cu Ka ($f' = -0.783$, $f'' = 7.348$) is still large enough to provide useful phase information, as a compromise between resolution limit and anomalous signal intensity, we selected the wavelength of 1.54 Å to collect the data for SAD phasing, while the data collection from native TCS crystal were done at wavelength of 0.98 Å for molecular replacement phasing.

The xenon was shown to bind to the pre-existing atomic-sized cavities in the interior of globular protein molecules [4]. The interaction of xenon atoms with proteins is the result of non-covalent, weak-energy van der Waals forces. Therefore, the process of xenon binding is completely reversible. As shown in Fig. 1(a), the Cα chain of native and Xe-derived TCS structures overlap exactly with each other (RMSD = 0.183 Å). The red sphere represents the location of xenon atom trapped inside of TCS. The residues forming xenon-binding cavity is enlarged in Fig. 1(b). A difference omit electron density map (Fig. 2) was calculated with $|F_{\text{obs, Xe}} - F_{\text{calc, Xe}}|$ using phases from the native structure. The map shows a strong peak (>16 sigma), corresponding to the xenon site.

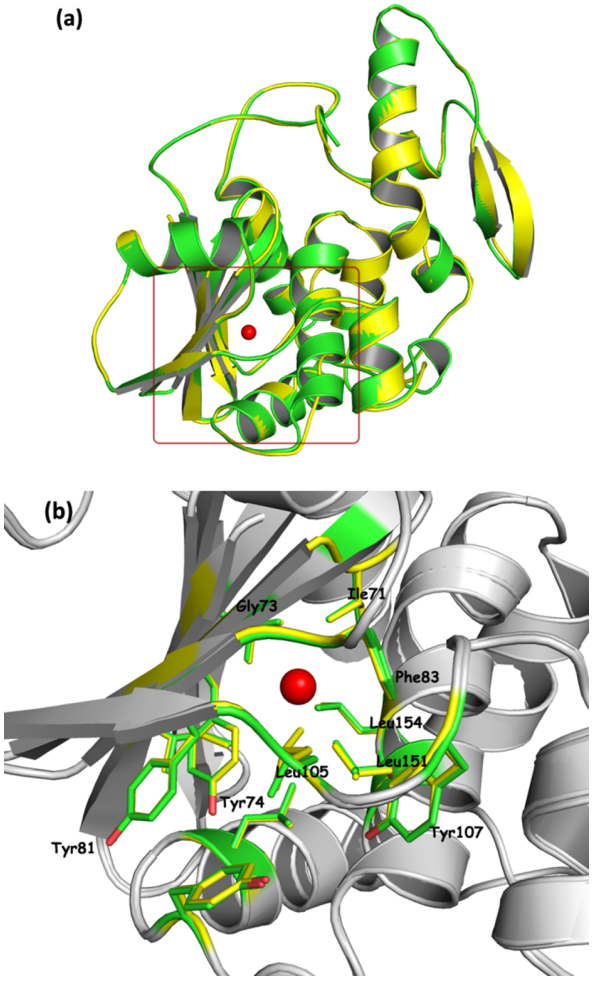

Fig. 1. (Color online) The superimposed structure models of trichonsanthin and Xe-derived trichosanthin (a). The native TCS structure is shown as yellow cartoon; the Xe-derived TCS structure is shown as green cartoon, and the Xenon atom is labeled as red ball. The RMSD of Cα chain of two structures is equal to 0.183 Å. The residues forming xenon-binding cavity is enlarged in Fig. 1(b).

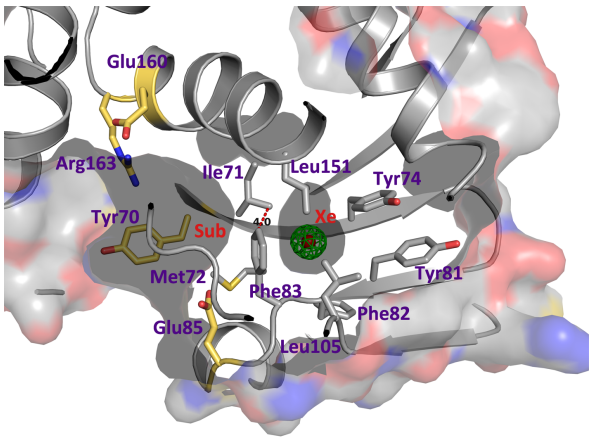

Fig. 2. (Color online) Difference omit map of Xenon atom site from Xe-derived trichosanthin. The green mesh indicates the F_{obs}–F_{calc} electron density of Xenon atom cut at 5σ; the peptide model is shown as gray cartoon; the Xenon atom is shown as red sphere; the residues forming the hydrophobic cavity for Xe-binding are shown as gray stick; the residues involving the substrate binding and catalyzing are shown as yellow stick. The dark surface marked as "Sub" indicates the substrate-binding pocket; the dark surface marked as "Xe" indicates the Xe-binding cavity.

The residues around the Xe atom are Ile 71, Met 72, Gly73, Tyr74, Tyr81, Phe82, Phe83, Leu105, and Leu151. Most of the residues possess hydrophobic side-chains. The distances between Xe atom and the atoms from the residues sit in the range of 3.2 Å to 5.0 Å (Table 2). It was reported that two putative hydrophobic sites existed inside TCS [17]. Different from them, the xenon-binding hydrophobic cavity here is relatively enclosed, with a volume in the same scale as xenon atom. Compared to the native TCS structure, no significant changes in the backbone or side chain conformation were observed upon binding Xe atoms, suggesting that there may be at least one pre-existing, inflexible hydrophobic cavity inside TCS for xenon binding. Because of its relatively small size, the cavity can accommodate only one single atom in a well-ordered position as the sphere electron density of xenon, as shown in Fig. 2.

C. The hypothetical xenon diffusion pathway inside TCS

Based on the TCS-NADHP complex structures [18], we can find that the substrate binding pocket of TCS (the dark surface marked as "sub" in Fig. 2) is adjacent to the Xe-binding cavity. Except the residues (Tyr70, Glu85, Glu160

TABLE 2. The distances between the Xenon atom and the atoms of protein residues forming the binding cavity in TCS.

Residue	Atom	Distance to Xe (Å)
ILE71	$C_{\gamma 2}$	4.67
GLY73	C_{α}	3.52
TYR74	$C_{\delta 1}$	4.03
TYR74	$C_{\varepsilon 1}$	4.53
TYR81	C_{β}	4.72
PHE82	C	4.27
PHE83	C_{ζ}	3.77
PHE83	$C_{\varepsilon 2}$	3.68
PHE83	$C_{\varepsilon 1}$	3.98
PHE83	$C_{\delta 1}$	4.09
PHE83	$C_{\delta 2}$	3.79
PHE83	C_{γ}	4.00
LEU105	C_{γ}	4.58
LEU105	$C_{\delta 1}$	3.43
LEU151	$C_{\delta 1}$	4.28
LEU151	$C_{\delta 2}$	4.02
LEU151	C_{γ}	4.82

TABLE 3. Xenon occupancy under multiple pressure and incubation time.

Pressure (MPa)	3	3	2	2	1	1
Time (min)	10	5	10	5	10	5
Number of Xe	1	1	1	1	1	1
Occupancy	0.54	0.48	0.45	0.43	0.35	0.35

and Arg163) involving in the substrate hydrolysis, two residues (Ile71 and Phe83) act as a set of "swing-door" to connect the protein surface to the hydrophobic core. Also, the smallest distance between the two residues is 4.0 Å, which is just enough to let the xenon atom to penetrate it, considering the van der Waals radius of Xe is 2.16 Å [4]. We propose that under the moderate pressure, xenon gas diffuses along the accessing channel to the bottom of the substrate-binding site, and squeezes into the hydrophobic cavity of Xe-binding site through the gate formed by residue Ile71 and Phe83.

The results of studies on the xenon complex with heme protein [8] showed the number and occupancies of xenon binding sites vary with the pressure applied. To estimate the possible xenon sites and the occupancies, three pressures (3 MPa, 2 MPa and 1 MPa) and two incubation duration (5 min and 10 min) were used with TCS crystals. However, from the datasets we collected (Table 3), only one xenon atom is located in Xe derivative structures, and the occupancy of Xe in the binding cavity does not gain obviously by increasing the pressure and incubation time. Perhaps further increase of the Xe gas pressure and incubation time shall be needed. Nevertheless, it might indicate from the other side that this xenon site is relatively conserved in TCS.

IV. CONCLUSION

In our report, we applied the noble gas xenon as "heavy atom" to solve the structure of protein trichonsanthin using SAD method. Compared to the native structure of TCS solved by molecular replacement in parallel, we located a conserved, inflexible hydrophobic Xe-binding cavity neighboring to its substrate binding site. Combined with the mica surface induced epitaxial crystal growth properties of TCS, we discovered that TCS would be a powerful and general applicable fusion tag in protein crystallography to solve the "unknown" protein structure especially in cases where selenomethionine incorporation may be difficult or impossible (i.e., in expression systems other than *E. Coli*).

[1] Schoenborn B P, Watson H C, Kendrew J C. Nature, 1965, **207**: 28–30.
[2] Schoenborn B P. Nature, 1965, **208**: 760–762.
[3] Vitali J, Robbins A H, Almo S C, *et al*. J Appl Crystallogr, 1991, **24**: 931–935.
[4] Schiltz M, Fourme R, Prange T. Method Enzymol, 2003, **374**: 83–119.
[5] Colloc'h N, Hajji M E, Bachet B, *et al*. Nat Struct Mol Biol, 1997, **4**: 947–952.
[6] Edwards P C, Li J, Burghammer M, *et al*. J Mol Biol, 2004, **343**: 1439–1450.
[7] Bourguet W, Ruff M, Chambon P, *et al*. Nature, 1995, **375**: 377–382.
[8] Luna V M, Chen Y, Fee J A, *et al*. Biochemistry-US, 2008, **47**: 4657–4665.
[9] Winter M B, Herzik M A, Kuriyan J, *et al*. P Natl Acad Sci USA, 2011, **108**: E881–E889.
[10] Hayakawa N, Kasahara T, Hasegawa D, *et al*. J Mol Biol, 2008, **384**: 812–823.
[11] Birukou I, Maillett D H, Birukova A, *et al*. Biochemistry-US, 2011, **50**: 7361–7374.
[12] Guskov A, Kern J, Gabdulkhakov A, *et al*. Nat Struct Mol Biol, 2009, **16**: 334–342.
[13] Wang Y. Pure Appl Chem, 1986, **58**: 789–798.
[14] Chow T P, Feldman R A, Lovett M, *et al*. J Biol Chem, 1990, **265**: 8670–8674.
[15] Shaw P C, Lee K M, Wong K–B. Toxicon, 2005, **45**: 683–689.
[16] Puri M, Kaur I, Perugini M A, *et al*. Drug Discov Today, 2012, **17**: 774–783.
[17] Zhou K, Fu Z, Chen M, *et al*. Proteins, 1994, **19**: 4–13.
[18] Xiong J P, Xia Z X, Wang Y. Nat Struct Mol Biol, 1994, **1**: 695–700.
[19] Sun L H, Xu C Y, Yu F, *et al*. Cryst Growth Des, 2010, **10**: 2766–2769.
[20] Otwinowski Z O and Minor W. Method Enzymol, 1997, **276**: 307–326.
[21] Sheldrick G. Acta Crystallogr A, 2008, **64**: 112–122.
[22] Wu L J, Zhang T, Gu Y X, *et al*. Acta Crystallogr D, 2009, **65**: 1213–1216.
[23] Winn M D, Ballard C C, Cowtan K D, *et al*. Acta Crystallogr D, 2011, **67**: 235–242.
[24] Cowtan K D, Zhang K Y J, Main P, *et al*., DM/DMMULTI software for phase improvement by density modification. In:

Arnold E and Arnold E editors. International Tables for Crystallography, Crystallography of Biological Macromolecules. Dordrecht, The Netherlands: Kluwer Academic Publishers, 2001, 407–412.
[25] Terwilliger T. J Synchrotron Radiat, 2004, **11**: 49–52.
[26] Langer G, Cohen S X, Lamzin V S, *et al*. Nat Protoc, 2008, **3**: 1171–1179.
[27] Murshudov G N, Vagin A A, Dodson E J. Acta Crystallogr D, 1997, **53**: 240–255.
[28] McCoy A J, Grosse Kunstleve R W, Adams P D, *et al*. J Appl Crystallogr, 2007, **40**: 658–674.
[29] Emsley P and Cowtan K. Acta Crystallogr D, 2004, **60**: 2126–2132.
[30] Adams P D, Afonine P V, Bunkoczi G, *et al*. Acta Crystallogr D, 2010, **66**: 213–221.